

Effects of Wind Speed on Quadcopter Ceiling Effect

Rhiannon Elliott-Roe*, Dr Kieran Wood, Dr Ozgun Ozer
 University of Manchester, Oxford Road, Manchester

ABSTRACT

The ceiling effect is an aerodynamic condition observed when a rotorcraft is in proximity of a horizontal, rigid surface above the rotors. It is in some ways like the ground effect, which has been well researched over the years both in the context of conventional helicopters and more modern quadcopters. This paper aims to investigate the ceiling effect and its impact on quadcopters in proximity flight, with a specific focus on whether there is a quantifiable difference in the thrust produced due to the ceiling effect in wind versus still air.

NOMENCLATURE

α_0, α_1	Dimensionless empirical constants which describe nonaxisymmetric flow and wake re-circulation.
T_{ICE}	Thrust in ceiling effect
T_{OCE}	Thrust out of ceiling effect
R	Radius of propeller
Z	Distance between propeller plane and artificial ceiling
\hat{z}	Z/R

1 INTRODUCTION

Unmanned Aerial Vehicles (UAVs) have been steadily growing in popularity since the mid-2010's as a tool for scientific research [1]. UAVs are typically limited by the battery capacity or the amount of fuel it can carry onboard, which can make it difficult to retrieve data from remote, inaccessible locations. Aerial rendezvous has the potential to increase the time-on-task for a data-gathering UAV by ferrying the UAV to its desired location via a larger parent vehicle with better endurance characteristics. The data-gathering vehicle in this case is a quadcopter, and the parent vehicle a fixed wing UAV. Once the data-gathering vehicle has performed its task, it first would then rendezvous with the parent UAV, which will take it back to the desired landing location. Addressing this problem requires an investigation into the disturbance effects of two vehicles flying in proximity.

*Email address: rhiannon.elliott@manchester.ac.uk

One of these proximity disturbances is known as the ceiling effect, which can be observed when the inflow through the propeller is obstructed to some degree by an overhead surface, which decreases the induced velocity across the rotor disk. This increases the thrust generated by the rotor, so it appears as if the quadcopter is being sucked up towards the overhead surface. In the context of aerial rendezvous, it is expected that a quadcopter could be forced into the wing of the parent vehicle, destabilising one or both UAVs. Evidently, this has the potential to cause catastrophic damage to the vehicle, the ceiling and any operators nearby, consequently, recent contributions to flight controller design have sought to sense and avoid the ceiling effect at all costs [2].

There is a strong need for research in proximity aerodynamics on small UAVs to aid the generation of mathematical models [3, 4]. These mathematical models are paramount for controller development and therefore reliable and predictable autonomous flight. Fully autonomous flight forms the foundation of operations which require faster responses than can be expected from a remote pilot; for example when flying in and around other UAVs or attempting complex manoeuvres such as mid-air rendezvous. As aircraft rendezvous is a complex and risk intensive process, the problem must be simplified. This may be done by modelling the underside of the wing as an infinite ceiling. This assumption would be appropriate when considering a small fixed wing quadcopter and a sufficiently large fixed wing UAV.

This paper aims to investigate the ceiling effect and its impact on thrust produced by a propulsion unit in proximity to an infinite ceiling. The focus of the experiment is to determine if wind speed causes a quantifiable difference in the thrust produced via ceiling effect. This will be done by first validating the experimental procedure against published theoretical models using a single rotor test case with no wind present. The test will then be repeated at different wind speeds.

2 LITERATURE REVIEW

One of the key examples of characterisation of rotor proximity interactions dates back to 1957, and discusses helicopters and the ground effect observed by pilots when coming into land. Although the idea of the ceiling effect was discussed, there was no interest to pursue this research due to the lack of operational requirement for helicopters to fly within such proximity to a rigid, overhead barrier. As UAV

technology develops, there is increasing interest in flight controllers that can safely navigate near large, rigid bodies [5].

“*The Effect of the Ground on a Helicopter Rotor in Forward Flight*” by Cheeseman and Bennett [6] focuses on the ground effect, an aerodynamic event that occurs when a helicopter approaches the ground and experiences an increase in thrust due to a cushion of air between the rotor plane and the ground. Cheeseman and Bennett put forward an approximate theory to estimate the thrust generated within ground effect, and how it changed with increasing forward airspeed. The findings from this paper suggested that the relative thrust increases as the distance between the rotor plane and the ground decreases, and that increasing forward speed decreases the relative thrust. This paper remains significant today and is featured in several pieces of literature that has been published in the last few years.

D Carter et al aimed to improve the design of near boundary flight controllers by investigating existing models for ground, ceiling and wall effects in “*Influence of the Ground, Ceiling and Sidewall on Micro-Quadcopters*” [7]. Through experimental testing, they were able to deduce that the theoretical models often over-predicted the thrust increase caused by the ceiling effect at small distances from the ceiling. This paper was of particular significance due to its Particle Image Velocimetry (PIV) studies which clearly illustrated the flow state around the propeller plane when in ceiling effect. Both the experimental validation of theoretical models, as well as PIV studies showing the complex inflow characteristics, have enriched the field of literature and gone on to aid further research on the ceiling effect.

In “*Multi-rotor UAS for Bridge Inspection by Contact using the Ceiling Effect*”, P Sanchez-Cuevas et al set out to capitalise on the ceiling effect by designing a protective fairing to shield the propellers on a quadcopter while maintaining the optimum distance between the ceiling and the rotor plane [5]. The optimum distance was determined using experimental methods like those discussed in [7] and was successfully validated by demonstrating the potential use as a bridge surveying tool. The quadcopter was able to remain attached to the ceiling at a reduced power setting as a direct result of the ceiling effect.

As perhaps one of the most significant works on ceiling effect, “*Ceiling Effects for Hybrid Aerial Surface Locomotion of Small Rotorcraft*” written by Hsiao et al explored the ceiling effect as a power conserving strategy [8]. By using Momentum Theory and Blade Element Method to complete a robust theoretical analysis of the phenomena, they were able to successfully generate a model for a quadrotor in ceiling effect as a function of blade radius, distance from

the ceiling and an empirical recirculation factor. While their model was verified using experimental testing, there are however limitations to the applications for other drones as the empirical constants would need to be determined for each drone type.

“*An Empirical Evaluation of Ground, Ceiling and Wall Effect for a Small-Scale Rotorcraft*” written by S Conyers et al; brings unique attention to the demands of the drone community for flying quadcopters indoors, and specifically that more work must be done to design flight controllers to fly within these complex flight regions rather than avoiding them entirely [2]. The authors propose that the ceiling obstructs the intake of the rotors, reducing the induced velocity of the flow and therefore increasing the thrust produced by the rotors for a given power setting. This is due to the inverse proportionality between thrust from the rotor and the induced velocity across the rotor disk, which can be shown when applying the conservation of momentum principle from far upstream of the propeller to far downstream. In addition to this, they address the uncertainty surrounding the validity of ceiling effect models that were initially based on ground effect models for single rotor helicopters. They suggest that the ceiling effect model can be applied to multi-rotors as the ceiling effect is an upstream phenomenon, whereas rotor wake interactions are a downstream phenomenon that should not interact with the ceiling effect to a significant extent.

Overall this section shows the accelerated pace at which research into the ceiling effect and how it interacts with quadcopters is being carried out. There is a noticeable shift in recent years where researchers aim to design flight controllers that can contend with the hazardous near-boundary flow of the ceiling effect, rather than minimising the time spent by the quadcopter in those regions. This paper aims to contribute to this research field by exploring how the ceiling effect may vary with wind speed. The findings from this research will support the development of proximity flight controllers which is a significant stepping stone along the path to reliable, autonomous aerial rendezvous.

3 THEORY

A low order modelling approach is adopted here to predict the ceiling effect in non-stationary conditions. The Hsiao and Chirarattananon model described in [8] and shown in 1, contains two empirically derived, dimensionless constants, α_0 and α_1 , to describe the non-axisymmetric flow and wake circulation respectively. Since this experiment will only consider a flat ceiling with respect to the rotor plane, the constant α_0 can be set to 1. Hsiao et al stated that where α_1 is assumed to be zero, for $\hat{z} > 0.05$ the model is still sufficiently accurate. Hence, substituting α_0 and α_1 to 1 and 0 respectively gives Equation 2.

$$\frac{T_{ICE}}{T_{OCE}} = \frac{1}{2} \left(1 - \frac{\alpha_1}{\hat{z}^2}\right) + \frac{1}{2} \sqrt{\left(1 - \frac{\alpha_1}{\hat{z}^2}\right)^2 + \frac{\alpha_0}{8\hat{z}^2}} \quad (1)$$

$$\frac{T_{ICE}}{T_{OCE}} = \frac{1}{2} + \frac{1}{2} \sqrt{1 + \frac{1}{8\hat{z}^2}} \quad (2)$$

Where $\hat{z} = Z/R$

Equation 1 has been verified experimentally for single rotor and quadcopter tests in [7, 9] and was found to have good agreement with theoretical data for the case where $\alpha_0 = 1$ and $\alpha_1 = 0$.

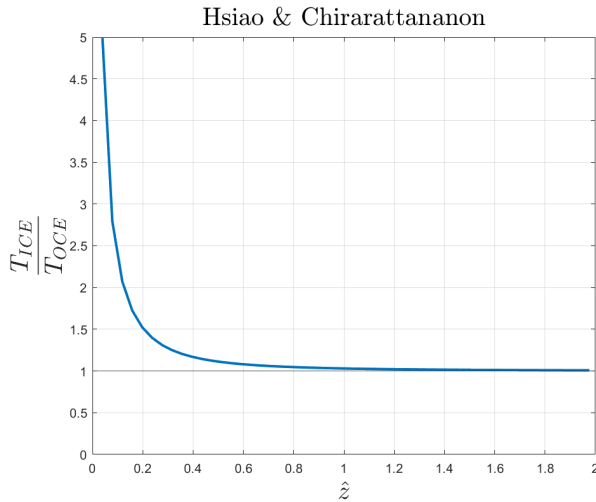


Figure 1: Hsiao and Chirarattananon Theoretical Model [8]

4 EXPERIMENTAL PROCEDURE

This section details the full experimental procedure for this paper including the apparatus, methodologies for both experiments and the data processing method. Initially, a single rotor test is carried out to verify the experimental data gathered agrees with the theoretical models published in the literature. The quadcopter data will be compared against the single rotor test as well as the theoretical model.

4.1 Apparatus

4.1.1 Wind Tunnel

This experiment was conducted in the open-circuit project wind tunnel at the University of Manchester, which can be seen in Figure 2. The test section is 1.2 x 0.9 x 2m and has a maximum speed of 50m/s [10] as shown in Figure 2.

Within the wind tunnel, the boundary layer forms before the test section begins. In the worst case scenario the boundary layer would be approximately 8.71mm according to the Blasius equation as seen in equation 2, and using the lowest wind speed of interest 10m/s [11]. To avoid interaction with the true ceiling boundary layer, the false ceiling will be suspended at least 50mm below the true ceiling to minimise the risk of boundary layer interaction from the true ceiling of the wind tunnel. The boundary layer formed on the artificial ceiling will be approximately 5.84mm thick at its maximum point which is acceptable as the closest the propeller will be to the ceiling is 15mm away.

$$\delta_{99}(x) \approx 5.0 \sqrt{\frac{\nu x}{u_0}} = 5.0 \frac{x}{\sqrt{Re_x}} \quad (3)$$

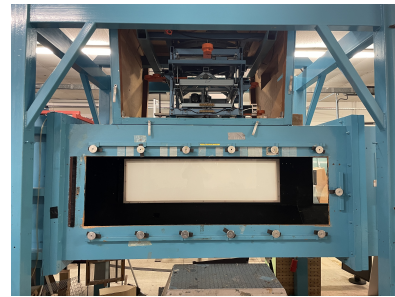


Figure 2: Project Wind Tunnel at the University of Manchester

4.1.2 Load Cell

A six-axis load cell (Mini40-E, ATI Industrial Automation, USA)[12] was used to collect measurements of the force and torques acting on the rotor and complete vehicle. The load cell is calibrated over a small range appropriate for the the up to 20 N forces predicted by theory.

4.1.3 Propulsion Unit

The experiment was conducted using an isolated propulsion unit. This unit is defined here as the entire power train required to convert electrical energy into useful work, hence; propeller (Holybro 1045), motor (Holybro 2216 920KV), and ESC (X500 V2 BLHeli S 20A). Power is provided by a 50 A bench supply to ensure experiments have a constant voltage input of 12V. A commutation RPM sensor was added (Hobbywing RPM Sensor) [13] between the motor and ESC, which was connected to a SpeedyBee F405 WING APP Fixed Wing Flight Controller [14] that recorded the rpm of the motor in the data logs.

http://www.imavs.org/

4.1.4 Motor stand

A telescopic speaker stand was used to vary the height between the artificial ceiling and the rotor plane. Adaptors were 3D printed using PLA so the propulsion unit could be fixed to the load cell, on top of the stand. The stand was required to move the rotor plane from 2 to 30cm away from the artificial ceiling, the minimum distance was set to 2cm to reduce the risk of the propeller blade striking the artificial ceiling. It was necessary to measure the distance between the rotor plane and the artificial ceiling without opening the wind tunnel. To do this, the motor stand was raised so that the rotor hub was just touching the artificial ceiling. From underneath the wind tunnel, the motor stand was marked where the bottom of the wind tunnel intersected with the stand. This point was marked as 0cm. The remaining markers were added from 2 to 30cm so that value intersecting the bottom of the wind tunnel represented the distance between the propeller and the ceiling. This allowed the distance between the rotor plane and the artificial ceiling to be adjusted without the need to open the wind tunnel. To prevent the speaker stand from moving during the experiment, slotted weights were used to weigh down the bottom of the tripod.

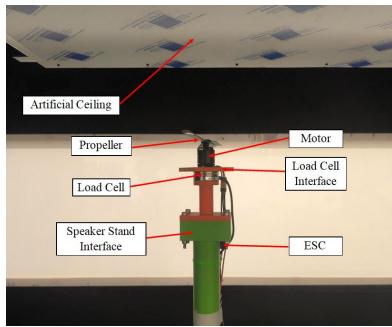


Figure 3: Annotated Picture of Single Motor on Test Stand

5 METHODOLOGY

The motor was controlled using a SpeedyBee F405 WING APP Fixed Wing Flight Controller [14] and the open-source program Mission Planner by ArduPilot. In Mission Planner, the motor test function allows the user to set the desired throttle percentage and test length in seconds. The RPM of the propeller was recorded using a commutation RPM sensor (Hobbywing RPM Sensor, [13]), with data being logged using the SpeedyBee Flight Controller. RPM was measured to verify that the propeller RPM was constant throughout the test, which was a key assumption in the theory set out by Hsiao et al [8].

The rotor axis was aligned with the z-axis of the load cell, so the force recorded by the load cell is equivalent to the thrust generated by the propulsion unit. The experiment was

started with no wind and the wind tunnel closed. Each data point taken represents five, five seconds long motor tests at a given throttle setting and distance. The distance between the propeller and the artificial ceiling was gradually increased from 2 to 30cm, in 1cm increments. Once the thrust and RPM data was recorded for each distance and throttle setting, the wind tunnel was turned on and the experiment was repeated at 5, 10 and 15m/s wind speed.

5.1 Data Processing

The load cell data was recorded directly using a LabView VI at a sampling rate of 10,000Hz. This data was then processed in MATLAB by using a 1D moving average filter, with a window size of 250 points to get an average thrust reading for each test. The average thrust reading was normalised by the Out-of-Ceiling effect thrust value which was taken at the maximum distance from the ceiling.

The RPM data was logged on the flight controller, then extracted and converted to a MATLAB file using Mission Planner. The mean RPM and the standard deviation was then calculated across each wind speed and throttle setting.

6 RESULTS

A range of throttle settings were used to investigate whether the normalised thrust was dependent on the throttle setting. The results at 0m/s are shown in Figure 4; each solid curve represents the fitted data at each wind speed and throttle setting. Figure 4 shows that there is no particular pattern which indicates throttle setting effects the normalised thrust produced. The same process was carried out at each subsequent wind speed, which also showed no link between throttle setting and thrust produced.

A key assumption in the theory described by Hsiao et al [8], was that RPM must remain constant at each distance away from the ceiling. In Table 1, the mean RPM and standard deviation as a percentage of RPM is shown. Overall, the standard deviation is low across the entire data set, which suggests that on the whole the RPM was maintained well. The larger standard deviations occur at wind speeds of 10 and 15 m/s, with the greatest deviation of 1.28% occurring at 55% throttle and 10m/s. It was observed during wind speeds of 10 and 15 m/s, that the propeller appeared to rock on the motor shaft. This rocking may cause inconsistencies with the RPM and would likely explain the greater deviation from the mean at higher wind speeds.

The propulsion unit was tested at 0, 5, 10 and 15 m/s wind speeds, and at 55%, 65% and 75% throttle, the results are shown in Figures 5, 6 and 7. The figures suggest that the normalised thrust data appears to follow the curve of theoretical thrust values (depicted in the figures with the

http://www.imavs.org/

Wind Speed [m/s]	Throttle Setting [%]					
	55		65		75	
	Mean RPM	Relative Standard Error	Mean RPM	Relative Standard Error	Mean RPM	Relative Standard Error
0	8043.067647	0.53%	9109.16	0.41%	10048.63	1%
5	8140.434532	0.42%	9235.253	0.46%	10207.88	1%
10	8125.405918	1.28%	9189.042	1.24%	10158.74	1%
15	8125.709903	1.27%	9189.31	1.24%	10158.89	1%

Table 1: Mean and Standard Deviation of RPM

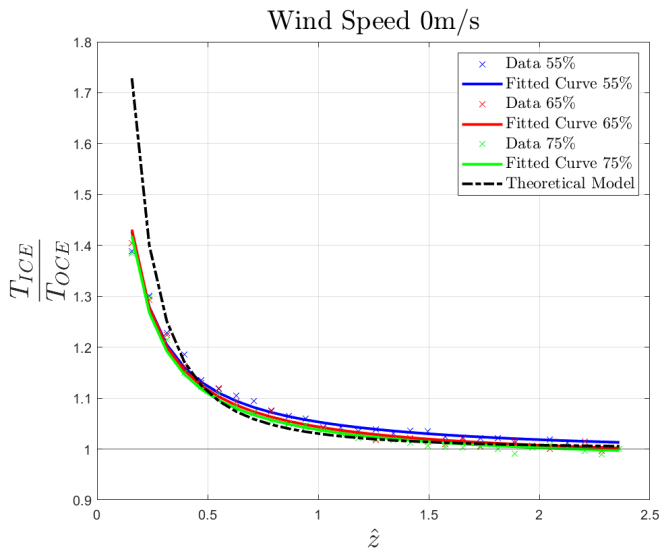


Figure 4: Normalised Thrust vs Normalised Distance From Ceiling for Propulsion Unit in 0m/s Wind

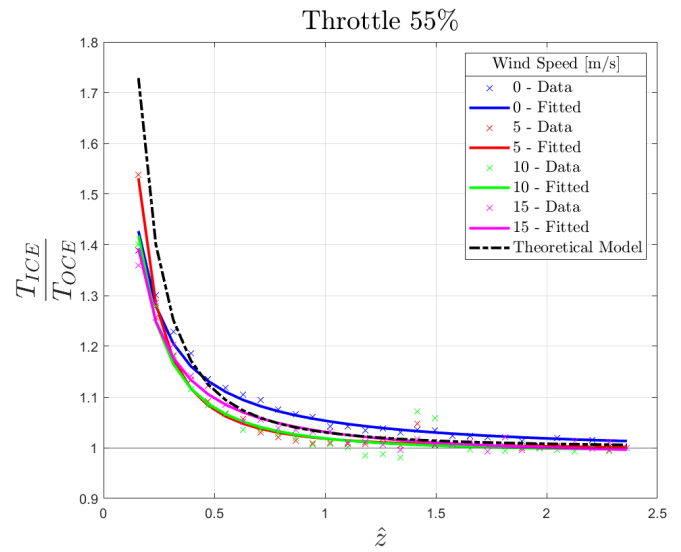


Figure 5: Normalised Thrust vs Normalised Distance From Ceiling for Propulsion Unit at 55% Throttle

dashed black line) as described by Equation 1 to some extent. However at normalised distances of 0.5 and less, the normalised thrust values appear to be less than that predicted by Equation 1.

To quantitatively evaluate the fit of these curves, the Mean Absolute Error for each data set was calculated, and is expressed in Table 6 as a percentage of the range of each data set. Overall, the Mean Absolute Error for each fit ranges from 3.689% to 8.226% which indicates that the data is loosely described by Equation 2, which was used as the model to fit the data against. The discrepancies between the experimental data and theoretical values at normalised distances less than 0.5 may explain why the Mean Absolute Error is as large as it is. There is no obvious trend as to whether the goodness of fit increases with either wind speed or throttle setting.

Figures 5, 6 and 7 show for each throttle setting, the normalised thrust at each different wind speed. If increasing

the wind speed decreased the thrust produced via ceiling effect, this would be shown by the curve shifting downwards on the y axis with increasing wind speed. This is not the case in these figures, as there is no consistent trend between the wind speed and normalised thrust produced in either Figure 5, 6 or 7. The figures and goodness of fit measurements shown suggest that wind speed does not cause a quantifiable difference in the thrust produced via ceiling effect for this specific configuration of propulsion unit and artificial ceiling.

7 DISCUSSION AND CONCLUDING REMARKS

This investigation into the ceiling effect and wind speed shows that with this configuration of propulsion unit and artificial ceiling, there is no quantifiable change in the thrust produced with varying wind speed. The normalised thrust values recorded during this experiment at 0m/s, are in good agreement with the results of [7, 8]. Notably how experimental values of normalised thrust are less than those predicted by the theory when \hat{z} approaches zero.

http://www.imavs.org/

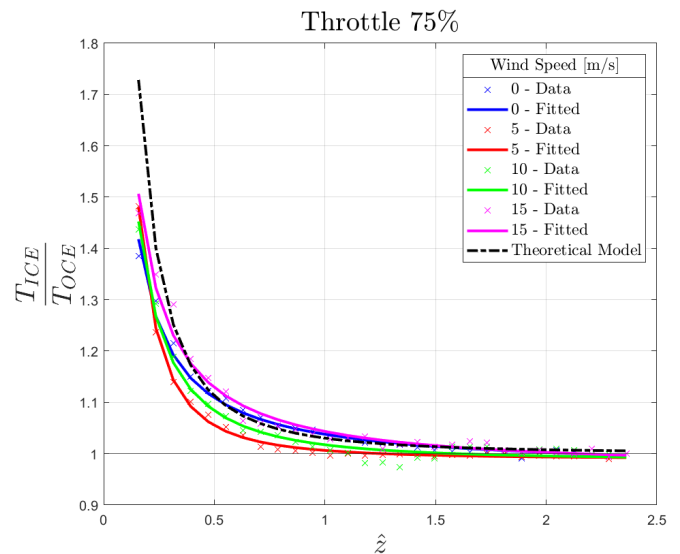
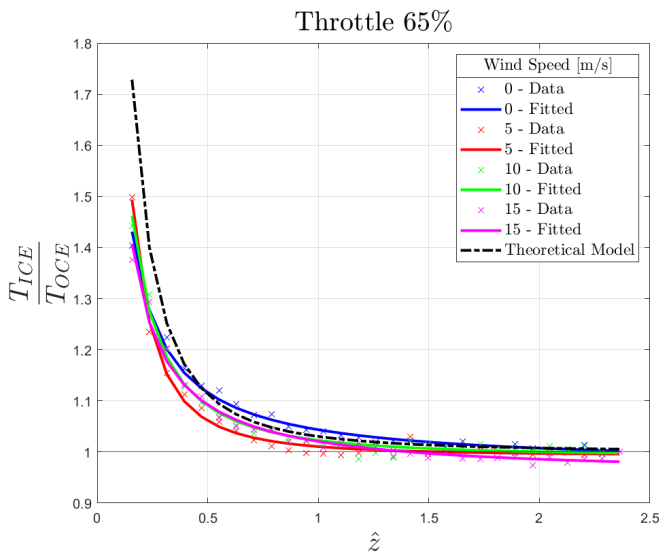


Figure 6: Normalised Thrust vs Normalised Distance From Ceiling for Propulsion Unit at 65% Throttle

Figure 7: Normalised Thrust vs Normalised Distance From Ceiling for Propulsion Unit at 75% Throttle

Wind Speed [m/s]	Mean Absolute Error as % of Range		
	Throttle 55%	Throttle 65%	Throttle 75%
0	7.297	5.279	5.371
5	4.806	7.077	8.226
10	7.572	5.338	6.633
15	6.293	8.054	3.689

Table 2: Mean Absolute Error Expressed as a Percentage of the Range

This suggests that the experimental procedure in the wind tunnel is valid for measuring the ceiling effect. The experimental method was not sufficient for ruling out whether wind speed has a quantifiable effect on ceiling effect for all cases. The phenomenon described by Cheeseman and Bennett in [6] which suggested that the ground effect decreased with increasing was in reference to helicopters which can fly much faster than a typical quadcopter. If these experiments were repeated at comparable wind speeds there may be a more obvious trend in the effect of wind speed on ceiling effect that mirror the results seen in [6].

These results are useful to the growing community of researchers exploring aerial rendezvous and proximity flight disturbances on UAVs [15]. Modelling the ceiling effect is key to developing controllers capable of anticipating aerodynamic disturbances such as the increase in thrust caused by the ceiling effect. In this specific case, the lack of relationship between the thrust increase due to ceiling effect and wind speed, means wind speed can effectively be ignored

when modelling this specific proximity flight disturbance. A less complex model may then make it easier to develop a controller for flying within proximity of overhead objects.

Further work must be done to address the limitations of this experimental model. The assumption that the propeller is parallel to the overhead ceiling would not hold in the real life situation where a quadcopter is flying at the speeds considered in this experiment, as quadcopters must have a non-zero pitch angle to move laterally. There are some examples in the literature of ceiling effect studies against non-parallel surfaces [16, 7, 4]. However, as none consider wind speed, this may be the next logical step in investigating whether wind speed has a quantifiable effect on the thrust produced in the ceiling effect.

REFERENCES

- [1] Anthony Harrington. Who Controls the Drones? *Engineering and Technology Magazine*, pages 80–83, 2015.
- [2] Stephen A. Conyers, Matthew J. Rutherford, and Kimon P. Valavanis. An Empirical Evaluation of Ground Effect for Small-Scale Rotorcraft. pages 1244–1250, 2018.
- [3] Derrick W Yeo, Nitin Sydney, Derek A Paley, and Donald Sofge. Downwash Detection and Avoidance with Small Quadrotor Helicopters. Technical report.
- [4] G. Throneberry, C. M. Hocut, and A. Abdelkefi. Multi-rotor wake propagation and flow development modeling: A review, 11 2021.

http://www.imavs.org/

- [5] P J Sanchez-Cuevas, Guillermo Heredia, and Anibal Ollero. *Multirotor UAS for Bridge Inspection by Contact Using the Ceiling Effect*. 2017.
- [6] I C Cheeseman and W E Bennett. The Effect of the Ground on a Helicopter Rotor in Forward Flight. Technical report, Ministry of Supply, Aeronautical Research Council Reports and Memoranda, London: Her Majesty's Stationery Office, 1957.
- [7] Darius J. Carter, Lauren Bouchard, and Daniel B. Quinn. Influence of the ground, ceiling, and sidewall on micro-quadrotors. *AIAA Journal*, 59(4):1398–1405, 2021.
- [8] Yi Hsuan Hsiao and Pakpong Chirarattananon. Ceiling Effects for Hybrid Aerial-Surface Locomotion of Small Rotorcraft. *IEEE/ASME Transactions on Mechatronics*, 24(5):2316–2327, 10 2019.
- [9] Basaran Bahadir Kocer, Tegoeh Tjahjowidodo, and Gerald Gim Lee Seet. Centralized predictive ceiling interaction control of quadrotor VTOL UAV. *Aerospace Science and Technology*, 76:455–465, 5 2018.
- [10] University of Manchester. Department of Mechanical, Aerospace and Civil Engineering Facilities, Wind Tunnels. <https://www.mace.manchester.ac.uk/research/facilities/wind-tunnels/>.
- [11] Marco Coderoni, Pankaj Rajput, Kalyan Goparaju, and Karthik Remella. Ansys Innovation Courses, Flat-Plate Blasius Solution - Lesson 4, 8 2020. <https://courses.ansys.com/index.php/courses/laminar-boundary-layer-theory/lessons/flat-plate-blasius-solution-ansys-innovation-courses/>.
- [12] ATI Industrial Automation. ATI F/T Mini40-E Load Cell. https://www.ati-ia.com/products/ft/ft_models.aspx?id=mini40.
- [13] HobbyWing USA. Hobbywing rpm sensor for high voltage esc. https://www.hobbywingdirect.com/products/rpm-sensor?srsltid=AfmBOocmlaWX46ehGaHFCp_QnILWY81NIsJFy2TQ33ClLXFCsWGE-S.
- [14] SpeedyBee. SpeedyBee F405 WING APP. <https://www.speedybee.com/speedybee-f405-wing-app-fixed-wing-flight-controller/>.
- [15] Sydney, Nitin and Smyth, Brendan and Paley, Derek A. Dynamic Control of Autonomous Quadrotor Flight in an Estimated Wind Field. pages 3609–3616, 2013.
- [16] Yuying Zou, Haotian Li, Yunfan Ren, Wei Xu, Yihang Li, Yixi Cai, Shenji Zhou, and Fu Zhang. Perch a quadrotor on planes by the ceiling effect.